SPMSMs Sensorless Torque Estimation Using High Frequency Signal Injection

David Reigosa†, Ye Gu Kang††, María Martínez†, Daniel Fernández†, J. M. Guerrero† and Fernando Briz†
†University of Oviedo. Dept. of Elect., Computer & System Engineering, Gijón, 33204, Spain.
†† University of Wisconsin-Madison, WEMPEC, Madison, WI-53706, USA
diazdavid@uniovi.es, ykang22@wisc.edu, martinezgmaria@uniovi.es, fernandezalodaniel@uniovi.es, guerrero@uniovi.es, fernando@isa.uniovi.es

Abstract: Torque measurement/estimation in surface permanent magnet synchronous machines (SPMSMs) is needed in many applications. Torque measurement systems are expensive, require extra room, add weight, can introduce resonances into the system, and their performance can be compromised due to electromagnetic interference. Alternatively, torque can be estimated, accurate knowledge of machine parameters being critical in this case. Injection of a high frequency (HF) signal in the stator via inverter has been shown to be a viable option for online identification of machine parameters identification required by torque estimation methods for interior PMSMs (IPMSMs). However, the reported methods require the use of two pulsating HF currents, which introduces concerns both on the adverse effects on machine's performance (additional noise, vibration, losses, …) as well as to the additional computational burden, as HF current controllers are required. This paper proposes a torque estimation method for SPMSMs using a single HF signal; further more, a HF voltage signal can be used, avoiding the use of HF current controllers, and therefore simplifying the implementation.[1]

Keywords—Permanent magnet synchronous machines, torque estimation, high frequency signal injection.

I. Introduction

Permanent magnet synchronous machines (PMSMs) are widely used in a large variety of high performance applications such as automotive, robotics, servo drive, military, aerospace…, due to their high efficiency, high power density and good dynamic response compared to other types of electrical machines [1]-[8]. Due to their importance, design, control, diagnostics and monitoring of PMSMs have been the focus of significant research efforts during the last decades.

Many applications require precise knowledge of machine torque [9]-[15]. Torque measurement systems can be roughly classified into strain gauges based methods [9]-[14] and torsional displacement based methods [15], with the first being the most extended. Both type of methods require extra room and cables, and their cost can account for a significant portion of the overall drive cost. Additionally, gauges based methods could introduce resonances into the system and are highly sensitive to electromagnetic interference. Torque estimation is often preferred due to these reasons [16]-[27].

Torque estimation methods can be roughly classified into torque equation based methods [16]-[18] and indirect estimation methods [19]-[27]. All these methods [16]-[27] require previous knowledge of certain machine parameters (PM flux, resistances, inductances…) and/or machine-operating condition (e.g. temperature), parameter sensitivity is one of the main weaknesses of these methods. To overcome this limitation, injection of pulsating HF signals on top of the fundamental excitation has been proved to be a viable option to estimate the machine parameters involved in the torque equation, i.e. PM flux and *dq*-axis inductances [18].

This paper proposes a new online parameter estimation method for SPMSMs aimed to improve the accuracy of torque estimation. The proposed method uses a modified torque equation based of HF parameters of the machine [28]. The parameters involved in the modified torque equation are estimated from the response to a HF signal injected in the stator terminals. While the method has some similarities with the method proposed in [18], the last required the injection of two pulsating HF currents, to estimate L_{dHF} (*d*-axis HF inductance), λ_{pm} (permanent magnet flux) and L_{qHF} (*q*-axis HF inductance) and implied therefore the use two HF current controllers. The method proposed in this paper requires the injection of only one HF signal, which can be either a voltage or current pulsating HF signal. This reduces the adverse effects of the HF signal on the performance of the machine and reduces the computational burden. A second difference with the method proposed in [18] is that this last used the conventional torque equation for torque estimation, while the method presented in this paper proposes a modification that will be shown to improve the torque estimation accuracy.

[1] This work was supported in part by the Research, Technological Development and Innovation Programs of the Spanish Ministry of Economy and Competitiveness, under grant MINECO-17-ENE2016-80047-R and by the Government of Asturias under project IDI/2018/000188 and FEDER funds.

The paper is organized as follows: fundamental model of a SPMSM is presented in section II, torque estimation using a HF signal is presented in section III, simulation and experimental results are presented in sections IV and V respectively, conclusions are finally provided in section VI.

II. Fundamental model of a PMSM

The general fundamental model of a PMSM in a reference frame synchronous with the rotor is given by (1) where R_d, R_q, L_d and L_q are the *d* and *q-axes* resistances and inductances respectively, ω_r is the rotor speed and λ_{pm} is the PM flux; *d*-axis being aligned with PMs. The output torque can be expressed as (2), where P is the number of poles, T_{syn} is the electromagnetic/synchronous torque and T_{rel} is the reluctance torque. In surface SPMSMs, due to their symmetric rotor structure, the differential inductance (L_d-L_q), i.e. saliency, is small [29]-[31] (≈7.8% for the test machine that will be used in this paper), meaning that $T_{syn} >> T_{rel}$; (2) can be also expressed as (3). It can be concluded from (2)-(3), that T_{out} estimation in SPMSMs requires estimation of λ_{pm}, L_d and L_q. It will be shown in the next section that all these parameters can be estimated from the response to a HF signal injected into the stator terminals of a SPMSM.

$$\begin{bmatrix} v_{sd}^r \\ v_{sq}^r \end{bmatrix} = \begin{bmatrix} R_d & 0 \\ 0 & R_q \end{bmatrix} \begin{bmatrix} i_{sd}^r \\ i_{sq}^r \end{bmatrix} + p \begin{bmatrix} L_d & 0 \\ 0 & L_q \end{bmatrix} \begin{bmatrix} i_{sd}^r \\ i_{sq}^r \end{bmatrix} + \begin{bmatrix} 0 & -\omega_r L_q \\ \omega_r L_d & 0 \end{bmatrix} \begin{bmatrix} i_{sd}^r \\ i_{sq}^r \end{bmatrix} + \begin{bmatrix} 0 \\ \lambda_{pm}\omega_r \end{bmatrix} \quad (1)$$

$$T_{out} = \frac{3}{2}\frac{P}{2}\left[\lambda_{pm} i_{sq}^r + \left(L_d - L_q\right) i_{sd}^r i_{sq}^r\right] = T_{syn} + T_{rel} \quad (2)$$

$$T_{out} = \frac{3}{2}\frac{P}{2}\left[(\lambda_{pm} + L_d i_{sd}^r) i_{sq}^r - (L_q i_{sq}^r) i_{sd}^r\right] \quad (3)$$

Flux observers reported in the literature for torque estimation, normally assume constant PM flux linkage λ_{pm} [32]-[33]. However, due to the temperature dependency of PMs' properties and saturation effect on the soft-iron, λ_{pm} varies, a linear relationship between torque and *q*-axis current not existing anymore [34]-[35]. Improvement of torque equation to include the variation of saturation level with temperature and fundamental current is presented in the next section. The *d*-axis HF inductance has been shown to be a reliable metric of the machine saturation level [36], and will be used for this purpose.

III. Torque estimation in SPMSMs using HF machine parameters

This section presents the HF model of a SPMSM and the physical principles of torque estimation in SPMSMs using HF signal injection.

a) *HF model of a SPMSM*

If the stator of a SPMSM is fed with a HF voltage/current sufficiently higher than the rotor frequency, the HF model shown in (4) can be deduced from (1) by neglecting the magnet flux (because it does not contain any HF component) and rotor speed dependent terms (assumed that the frequency of the HF signal is sufficiently higher than the rotor frequency [36]-[38]), where v_{sdHF}^r and v_{sqHF}^r are the *dq*-axes HF voltages in the rotor reference frame, i_{sdHF}^r and i_{sqHF}^r are the *dq*-axes HF currents in the rotor reference frame, and L_{dHF} and L_{qHF} are the *dq*-axes HF inductances. Furthermore, if the frequency of the HF signal is high enough, the HF resistive term can be safely neglected compared to the inductive term.

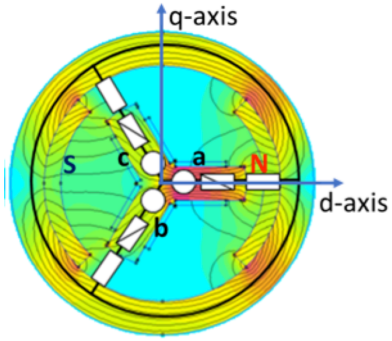

Fig. 1.- 2-pole 3-slot equivalent magnetic circuit of a SPMSM.

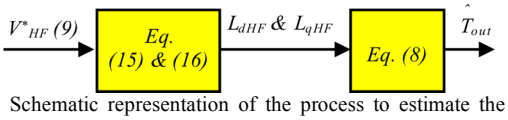

Fig. 2.- Schematic representation of the process to estimate the output torque using pulsating HF voltage injection.

In an stationary reference frame (i.e. stator reference frame), the HF model shown in (4), is expressed by (5), where ΣL and ΔL are the mean and differential inductances respectively, (6) and (7), θ_r is the rotor electrical position, v_{sdHF}^s and v_{sqHF}^s are the *dq*-axes HF voltages in the stator reference frame and i_{sdHF}^s and i_{sqHF}^s are the *dq*-axes HF currents in the stator reference frame.

$$\begin{bmatrix} v_{sdHF}^r \\ v_{sqHF}^r \end{bmatrix} = p \begin{bmatrix} L_{dHF} & 0 \\ 0 & L_{qHF} \end{bmatrix} \begin{bmatrix} i_{sdHF}^r \\ i_{sqHF}^r \end{bmatrix} \quad (4)$$

$$\begin{bmatrix} v_{sdHF}^s \\ v_{sqHF}^s \end{bmatrix} = \begin{bmatrix} \Sigma L - \Delta L\cos(2\theta_r) & -\Delta L\sin(2\theta_r) \\ -\Delta L\sin(2\theta_r) & \Sigma L + \Delta L\cos(2\theta_r) \end{bmatrix} \begin{bmatrix} i_{sdHF}^s \\ i_{sqHF}^s \end{bmatrix} \quad (5)$$

$$\Sigma L = \frac{L_{dHF} + L_{qHF}}{2} \quad (6)$$

$$\Delta L = \frac{L_{qHF} - L_{dHF}}{2} \quad (7)$$

b) *Torque estimation in SPMSMs using HF signal injection*

The modified torque equation obtained from (2)-(3) is shown in (8). It is observed from (8) that the estimated *d*-axis HF inductance is used to scale the nominal PM flux linkage, λ_{pm0}. The *d*-axis HF inductance is function of the *d*-axis reluctance variation, reflecting therefore saturation effect on *d*-axis. Fig. 1 shows a simplified representation of the equivalent magnetic circuit of a 2-pole 3-slot SPMSM; this machine configuration has been used for exemplification purposes due to its simple structure. The equivalent magnetic circuit is composed of: three phase coils, represented by abc flux source,

variable reluctance components on the soft-iron taking into account saturation effect and PM generate flux; the PM flux path being aligned with the *d*-axis. It can be concluded that, for an SPMSM, the saturation effect on *d*-axis HF inductance is function of the PM flux linkage operating point; a linear relationship between *d*-axis HF inductance and PM flux linkage operating point has been assumed in this case. This relationship was achieved on an empirical basis, development of a mathematical model is a subject of ongoing current research.

$$T_{out} = \frac{3}{2}\frac{P}{2}\left[(\lambda_{pm0}\frac{L_{dHF}}{L_{dHF0}} + L_{dHF} i^r_{sd}) i^r_{sq} - \left(L_{qHF} i^r_{sq}\right) i^r_{sd} \right] \quad (8)$$

where λ_{pm0} and L_{dHF0} are the PM flux and *d*-axis HF inductance at the room temperature (T_{r0}) and when no *dq*-axes fundamental current is injected.

Fig. 2 shows schematically the implementation of the proposed method. The HF voltage is injected superimposed on top of the fundamental voltage. HF inductances are estimated from the commanded HF voltage and the resulting HF current. Finally, the estimated *d*-axis HF inductance is used for scaling the PM flux linkage to improve the real-time torque estimation. Since *d* and *q*-axis HF inductances are estimated online, variations due to changes of PM temperature or *d* and *q*-axis current levels [18] do not affect to the accuracy of the method.

c) HF inductance estimation in SPMSMs using HF signal injection

If a pulsating HF voltage is injected in the stator terminals of the machine (9), the resulting HF current is represented by (12), where V^*_{HF} is the magnitude of the injected HF signal, θ_{HF} is the phase of the HF signal (10), ω_{HF} is the frequency of the HF signal, $\hat{\theta}_r$ is the injection angle of the pulsating HF voltage (11) and φ is an arbitrary angle; e.g. if φ=0 the pulsating HF voltage will be injected in the *d*-axis of the machine, while if φ=π/2 it will be injected in the *q*-axis. In the injection reference frame, (12) is transformed into (13).

$$\begin{bmatrix} v^{s*}_{dsHF} \\ v^{s*}_{qsHF} \end{bmatrix} = V^*_{HF}\sin(\theta_{HF}) \begin{bmatrix} \cos(\hat{\theta}_r) \\ \sin(\hat{\theta}_r) \end{bmatrix} \quad (9)$$

$$\theta_{HF} = \omega_{HF} t \quad (10)$$

$$\hat{\theta}_r = \theta_r + \varphi \quad (11)$$

$$\begin{bmatrix} i^s_{sdHF} \\ i^s_{sqHF} \end{bmatrix} = \frac{V^*_{HF}}{\omega_{HF}\left(\Sigma L^2 - \Delta L^2\right)} \begin{bmatrix} \Sigma\cos(\hat{\theta}_r) + \Delta L\cos(2\theta_r - \hat{\theta}_r) \\ \Sigma\sin(\hat{\theta}_r) + \Delta L\sin(2\theta_r - \hat{\theta}_r) \end{bmatrix} \quad (12)$$

$$\begin{bmatrix} i^{\hat{\theta}_r}_{sdHF} \\ i^{\hat{\theta}_r}_{sqHF} \end{bmatrix} = \frac{V^*_{HF}}{\omega_{HF}\left(\Sigma L^2 - \Delta L^2\right)} \begin{bmatrix} \Sigma L + \Delta L\cos(2(\theta_r - \hat{\theta}_r)) \\ \Delta L\sin(2(\theta_r - \hat{\theta}_r)) \end{bmatrix} \quad (13)$$

If the HF is injected between *d* and *q*-axes, i.e. $\hat{\theta}_r = \theta_r + \pi/4$, (13) can be simplified into (14) [39]. Having two equations and two unknowns, L_{dHF} and L_{qHF}, the HF inductances can be estimated from (15) and (16).

TABLE 1. MACHINE PARAMETERS

P_{rated} [kW]	I_{rated} [A]	k_t [Nm/A]	Poles	ω_{rated} [rpm]
6.6	15	4.2	8	1000

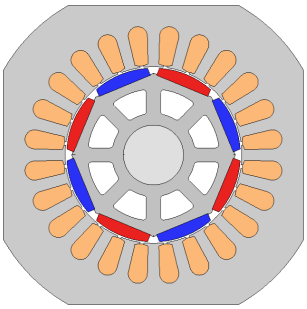

Fig. 3.- Schematic representation of the test machine.

$$\begin{bmatrix} i^{\hat{\theta}_r}_{sdHF} \\ i^{\hat{\theta}_r}_{sqHF} \end{bmatrix} = \frac{V^*_{HF}}{\omega_{HF}\left(\Sigma L^2 - \Delta L^2\right)} \begin{bmatrix} \Sigma L + \Delta L\cos(-\pi/2) \\ \Delta L\sin(-\pi/2) \end{bmatrix} = \frac{V^*_{HF}}{\omega_{HF}\left(\Sigma L^2 - \Delta L^2\right)} \begin{bmatrix} \Sigma L \\ -\Delta L \end{bmatrix} \quad (14)$$

$$L_{dHF} = \frac{V^*_{HF}}{\omega_{HF}\left(i^{\hat{\theta}_r}_{sdHF} - i^{\hat{\theta}_r}_{sqHF}\right)} \quad (15)$$

$$L_{qHF} = \frac{V^*_{HF}}{\omega_{HF}\left(i^{\hat{\theta}_r}_{sdHF} + i^{\hat{\theta}_r}_{sqHF}\right)} \quad (16)$$

IV. FEM results

Finite element analysis (FEA) simulation results are presented in this section to validate the proposed method. Fig. 3 shows a schematic representation of the SPMSM that will be used; Table 1 shows the parameters of the machine. Fig 4 shows simulations results changing both I_d and I_q currents from -15A (-1 pu) to 15A (1 pu), in steps of 1.5 A, half of the operating points in flux-weakening region (I_d <0) and half in flux-intensifying region (I_d >0). A HF voltage signal of 10V and 250Hz, injected between *d* and *q*-axes (i.e. $\hat{\theta}_r = \theta_r + \pi/4$), is used for all FEA simulation results.

Fig. 4a and 4b shows the estimated *d* and *q*-axes HF inductances. It is observed that the *d*-axis inductance is smaller than *q*-axis inductance due to saturation, which is an expected result. Also, it can be noticed that the *d*-axis inductance is more prone to the armature current since the *d*-axis flux path is biased with PM flux source; it is important to note that the armature current flux path in *d*-axis is shared with PM flux path. The saturation level of *d*-axis flux path is indirectly estimated in the form of *d*-axis HF inductance in real-time for dynamic torque estimation.

Fig. 4c-e show the measured torque (T_{meas}), the estimated torque using the general torque equation (3) (T_{out_conv}) and the estimated torque using the proposed method (8) (T_{out_HF}), note that the HF inductances shown in Fig. 4a and 4b are used for torque estimation when using the proposed method, see (8).

Fig. 4f and 4g show the torque estimation error when using the general torque equation and when using the proposed

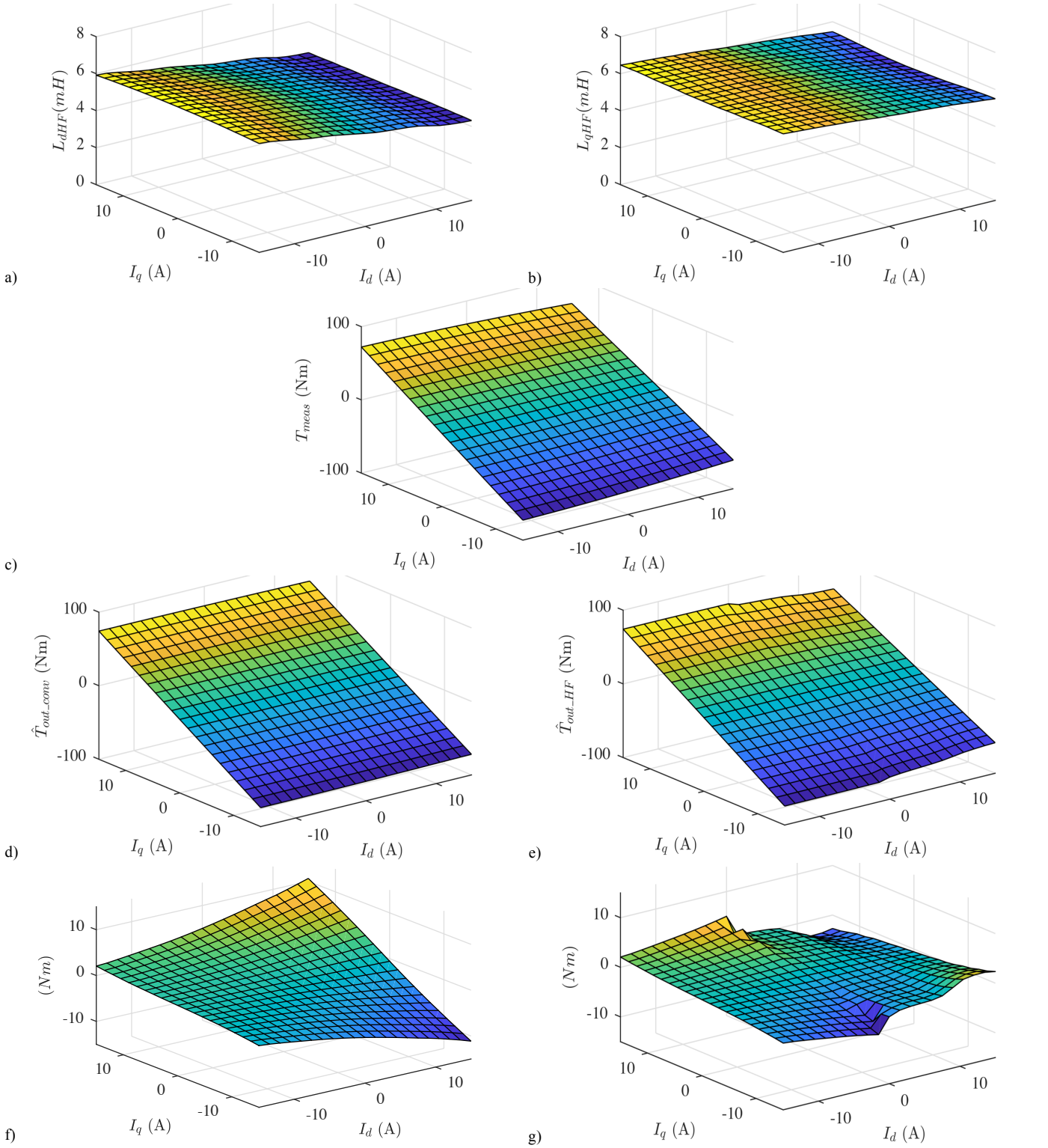

Fig. 4.- FEA results. a) Estimated *d*-axis HF inductance (15), b) estimated *q*-axis HF inductance (16), c) measured torque, d) estimated torque using the general torque equation (3), e) estimated torque using proposed method (8), f) torque estimation error usign the general torque equation and g) torque estimation error using the proposed method. V_{HF}=10 V, f_{HF}=250Hz, ω_r=2·π·66 rad/s, , -15A<I_d<15A, -15A<I_q<15A.

method respectively. It is observed that the toque estimation error when using the proposed method is <4Nm (0.05 pu), while it is <11Nm (0.137 pu) when using the general torque equation; the maximum of the torque estimation error when using (3) occurs in the heavily saturated region (e.g. I_d and $|I_q|$>0.8 pu), the proposed technique improves the estimation in this region. This is because the general torque equation assumes constant PM flux linkage and *dq*-axis inductances (see (3)), while the

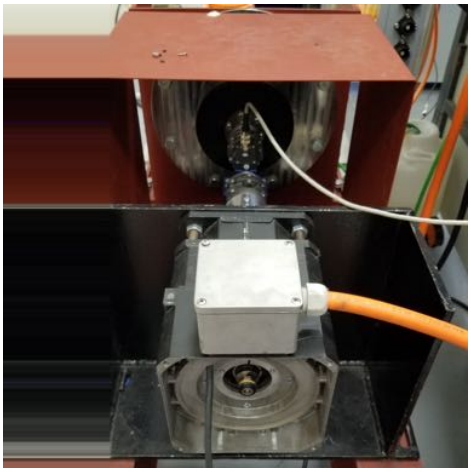

Fig. 5.- Experimental setup with test SPMSM, torque sensor, and axial PMSM for the load machine.

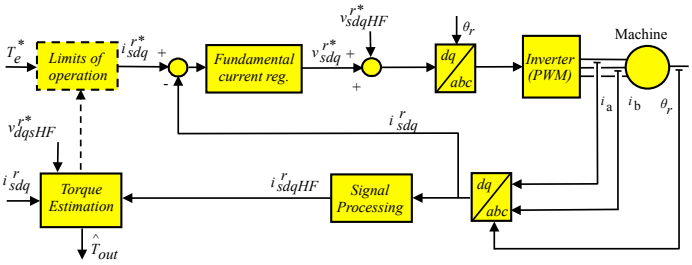

Fig. 6.- Injection of pulsating HF voltage. Dashed lines indicate optional functionalities.

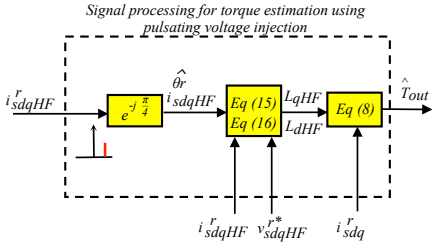

Fig. 7.- Schematic representation of the signal processing for torque estimation using pulsating HF voltage injection.

proposed method dynamically adapt these parameters from the response to the injected HF signal.

V. Experimental results

Experimental results are shown in this section. Fig. 5 shows the experimental setup. The test SPMSM is the same describe in Section IV. It is loaded with an axial PMSM (EMRAX 228 [40]) driven by a *BAMOCAR-PG-D3* power converter [41]; the setup including an Interface T3 torque sensor [42]. A HF voltage signal of 10V and 250Hz, injected between *d* and *q*-axes (i.e. $\hat{\theta}_r = \theta_r + \pi/4$), is used for all experimental results.

Fig. 6 shows the general control block diagram of the machine while Fig. 7 shows the signal processing required for the torque estimation. As already stated, the pulsating HF voltage, v^{r*}_{sdqHF}, is injected between *d* and *q*-axis, the resulting HF current, i^{s}_{sdqHF}, containing information of the inductances of the machine. *Dq*-axis inductances are obtained using (15) and (16). The torque is finally estimated using (8). It can be

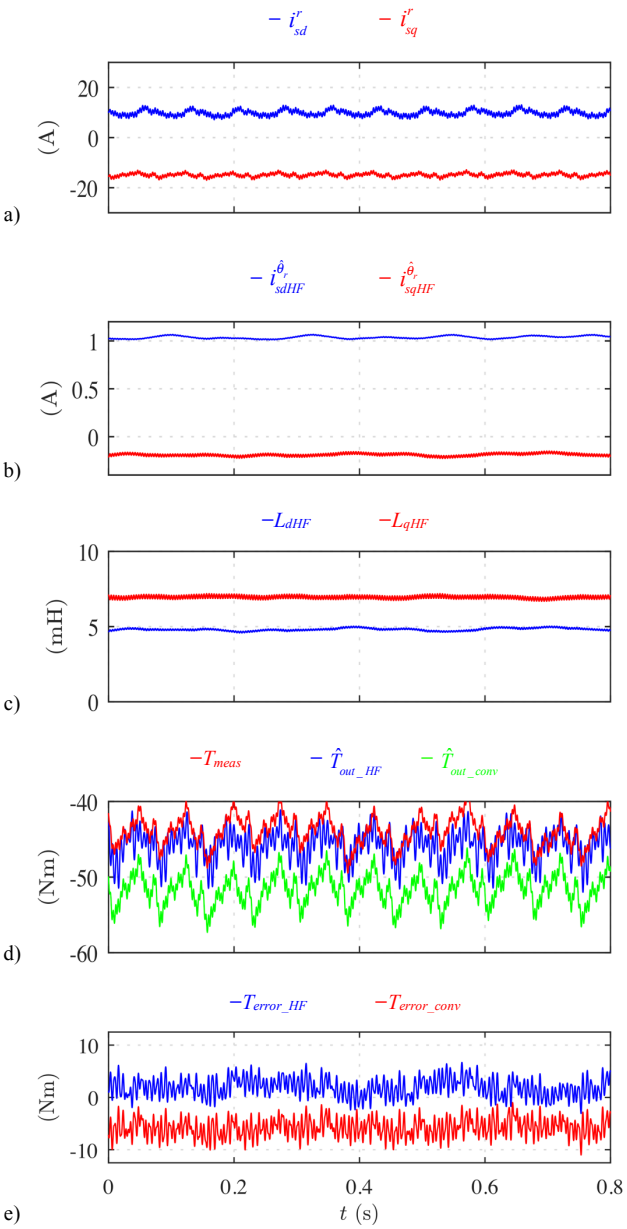

Fig. 8. – Experimental results. a) *dq*-axes currents, b) magnitudes of the *dq*-axes HF currents (14), c) *dq*-axes HF inductances, d) measured and estimated torque and e) torque error. I_d = 10A and I_q = -15A, V_{HF}=10V, f_{HF} = 250Hz, ω_r=2· π ·66 rad/s.

observed from Fig. 6 that knowledge of rotor position is required. For the experimental results shown in the paper an encoder with 4096 ppr has been used. Simultaneous use of HF signal injection for rotor position estimation and torque estimation should be feasible, but has not been investigated yet.

Fig. 8a shows the *d* and *q*-axes fundamental currents when the test machine is operated with positive *d*-axis current, i.e. flux-intensifying current (10A). Fig. 8b shows the *d* and *q*-axes HF currents, see (14); a band pass filter of 100Hz being used to isolate the HF currents. Fig. 8c shows the estimated HF inductances using (15) and (16). It is observed from Fig. 8c that the *d*-axis HF inductance is smaller than the *q*-axis HF inductance due to saturation, which was an expected result

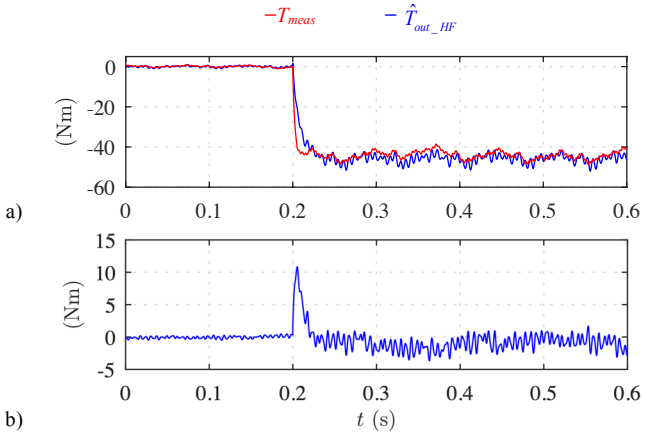

Fig. 9. – Experimental results. a) measured and estimated torque and b) torque error when a q-axis current step, 0 to -15A, is applied at t=0.2s. I_d = 10A, V_{HF}=10V, f_{HF} = 250Hz, ω_r=2·π·66 rad/s.

since the machine is being operated in the flux-intensifying region. Fig. 8d shows the measured torque using the torque sensor [45] (T_{meas}), the estimated torque using the general torque equation (3) ($\hat{T}_{out\_conv}$) and the estimated torque using the proposed method (8) ($\hat{T}_{out\_HF}$).

Finally, Fig. 8e shows the torque estimation error using both, the general torque equation and the proposed method; the reduction of its mean value (continuous torque) for the second being evident.

Fig. 9 shows the response to a step-like q-axis current command. Fig. 9a shows the measured torque and the estimated torque using the proposed method (8), while Fig. 9b shows the torque estimation error. It is observed that the dynamic response of the estimation is in the range of miliseconds.

Fig 10 shows experimental results of the proposed method for different I_d-I_q working conditions. Fig. 10a and b shows the estimated d and q-axes HF inductances; it is noted that the results in Fig. 10a and 10b are in good agreement with the simulation results, see Fig. 4.

Fig. 10c-e show the measured and estimated torques using the general torque equation (3) and the proposed method (8) respectively, Fig. 10f and 10g showing the corresponding estimation errors. SMSMs are typically operated with $I_d \leq 0$. Torque estimation error in this region using the proposed method is reduced by ≈50% with respect to the conventional method. Maximum error using both the conventional and the proposed method occurs when the machine is heavily saturated (I_d & I_q >0.8 pu); still there is a reduction of the error in the range of ≈50% using the proposed method. It must be noted that operation with large positives values of I_d (flux intensifying region) is unusual in SPMSMs.

Finally, Fig. 11 shows experimental results using the proposed method vs. I_d&I_q for three different speeds. It can be observed that the torque estimation error slightly increases as the speed decreases.

VI. Conclusions

This paper proposes a new online parameter estimation method for SPMSMs aimed to improve the accuracy of torque estimation. The proposed method uses a modified torque equation based of HF parameters of the machine. The parameters involved in the modified torque equation are estimated from the response to a HF signal injected in the stator terminals. The HF signal is superposed on top of the fundamental excitation, allowing therefore real time torque estimation without interfering with the normal operation of the machine. FEA simulation results and experimental results injecting a HF voltage signal have been provided to demonstrate the viability of the proposed method. It has been shown that the proposed method improves the torque estimation compared to the general torque equation method.

VII. References

[1] Duane C. Hanselman, "Brushless Permanent Magnet Motor Design" New York: Mc-Graw Hill, 1994.

[2] B. Saunders, G. Heins, F. De Boer and M. Thiele, "Cogging torque estimation for sensorless PMSM," International Conference on Electrical Machines (ICEM), 2949-2954, Sept. 2012.

[3] Fukushige, N. Limsuwan, T. Kato, K. Akatsu, and R. D. Lorenz, "Efficiency contours and loss minimization over a driving cycle of a variable flux-intensifying machine,"IEEE Trans. Ind. Appl., 51(4): 2984–2989, Jul./Aug. 2015

[4] J. F. Gieras and M. Wing, "Permanent magnet motor technology: design and application". Second edition 2002.

[5] W. Xu and R. D. Lorenz, "High-Frequency Injection-Based Stator Flux Linkage and Torque Estimation for DB-DTFC Implementation on IPMSMs Considering Cross-Saturation Effects," IEEE Transactions on Industry Applications, 50(6): 3805-3815, Nov.-Dec. 2014.

[6] M. Piccoli, and M. Yim. "Cogging Torque Ripple Minimization via Position Based Characterization." Robotics: Science and Systems, 2014.

[7] O. Pyrhonen and P. Eskelinen, "Advanced measurement of rotor vibration in electric drives." IEEE Aerospace and Electronic Systems Magazine, vol.13, no. 5, pp. 21-23, May 1998.

[8] J. C. Urresty, R. Atashkhooei, J. R. Riba, L. Romeral and S. Royo, "Shaft Trajectory Analysis in a Partially Demagnetized Permanent-Magnet Synchronous Motor." IEEE Transactions on Industrial Electronics, vol. 60, no. 8, pp. 3454-3461, Aug. 2013.

[9] http://www.interfacetorque.co.uk

[10] https://www.hbm.com

[11] http://www.futek.com

[12] http://www.magtrol.com/torque

[13] http://www.te.com

[14] G. Heins, M. Thiele and T. Brown, "Accurate Torque Ripple Measurement for PMSM" IEEE Transactions on Instrumentation and Measurement, 60(12): 3868-3874, Dec. 2011.

[15] P. Sue, D. Wilson, L. Farr and A. Kretschmar, "High precision torque measurement on a rotating load coupling for power generation operations," IEEE International Instrumentation and Measurement Technology Conference Proceedings, pp. 518-523, May 2012.

[16] K. C. Yeo, G. Heins and F. De Boer, "Comparison of torque estimators for PMSM," AUPEC, pp. 1-6, 2008.

[17] B. Cheng and T. R. Tesch, "Torque Feedforward Control Technique for Permanent-Magnet Synchronous Motors", IEEE Trans. on Ind.Electr., 57(3): 969-974, March 2010.

[18] M. Martinez, D. Reigosa, D. Fernandez, J.M. Guerrero and F. Briz, "PMSMs Torque Estimation Using Pulsating HF Current Injection", IEEE-SLED, pp. 96-101, Sept. 2018.

[19] F. Jukic, D. Sumina and I. Erceg, "Comparison of Torque Estimation Methods for Interior Permanent Magnet Wind Power Generator", IEEE EDPE, pp. 291-296, Oct. 2017.

[20] Weizhe Qian, S.K. Panda, and Jian-Xin Xu, "Improved PMSM pulsating torque minimization with iterative learning and sliding mode observer", IECON, pp. 1931-1936, 2000.

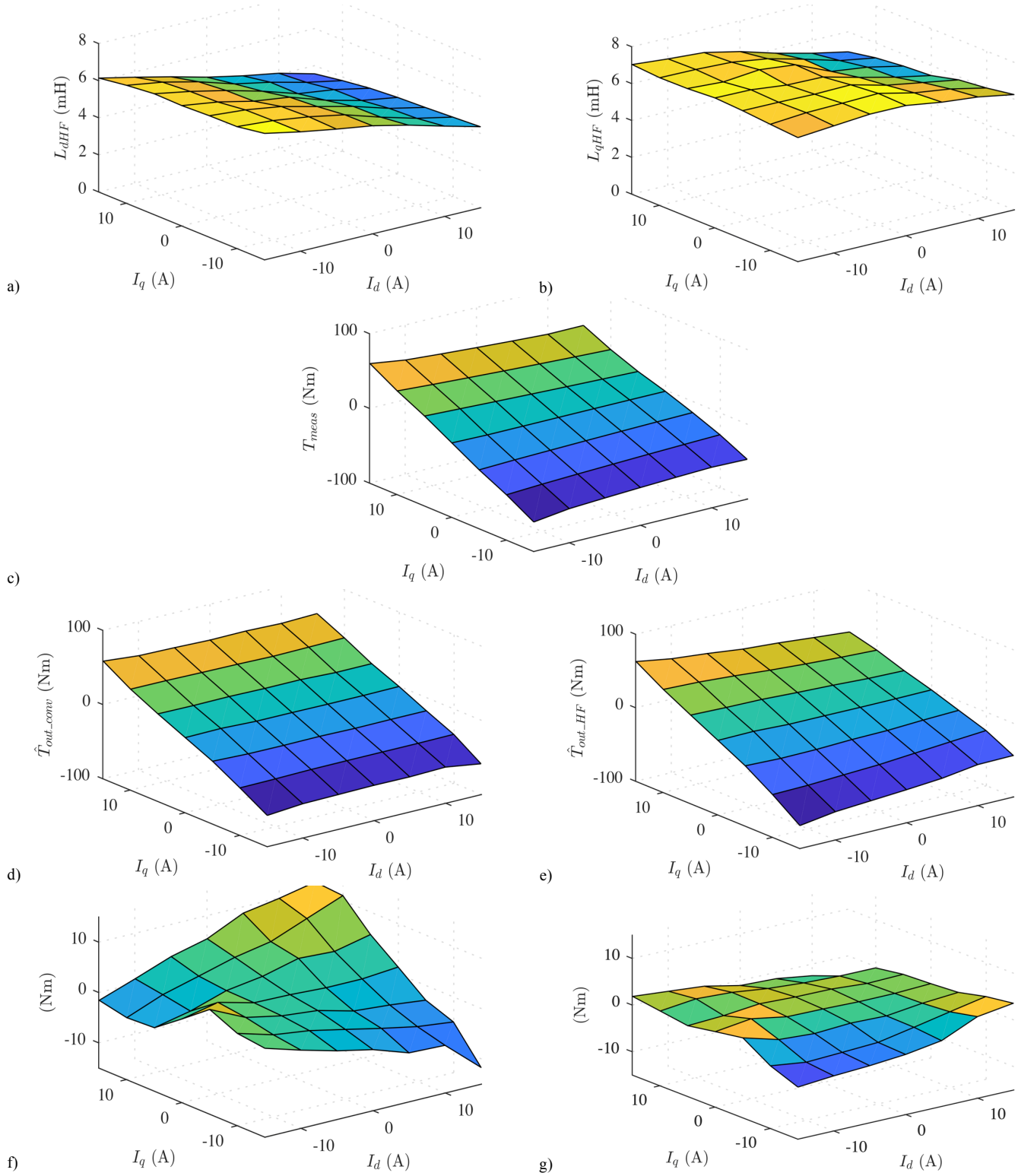

Fig. 10.- Experimental results. a) Estimated *d*-axis HF inductance (15), b) estimated *q*-axis HF inductance (16), c) Measured torque, d) estimated torque using the general torque equation (3), e) estimated torque using proposed method (8), f) torque estimation error usign the general torque equation and g) torque estimation error usign the proposed method. V_{HF}=10V, f_{HF}=250Hz, ω_r=2·π·66 rad/s.

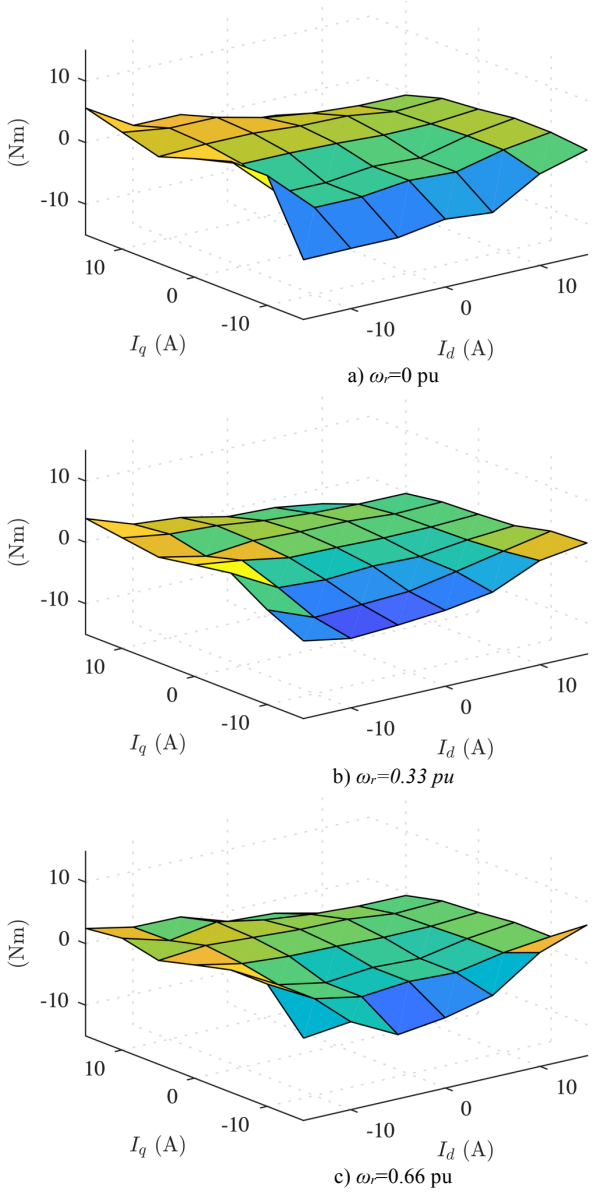

a) ω_r=0 pu

b) ω_r=0.33 pu

c) ω_r=0.66 pu

Fig. 11. – Experimental results. Torque estimation error vs. I_d & I_q using the proposed method for three different speeds. V_{HF}=10V, f_{HF}=250Hz.

[21] B. H. Lam, S. K. Panda, J. x. Xu and K.W. Lim 'Torque ripple minimization in PM synchronous motor using iterative learning control', IEEE PED, pp. 141-149, 1999.

[22] S. -K. Chung, H. -S. Kim, C. -G. Kim and M. -J. Youn, 'A new instantaneous torque control of PM synchronous motor for high-performance direct drive applications', IEEE Trans. Power Elect., 13(3): 388-400, May 1998.

[23] Xu Dong and Wang Tianmiao and Wei Hongxing, "Comparison between model reference observer and reduced order observer of PMSM torque", IEEE-ICIEA, pp. 663-667, 2011.

[24] Q. Liu and K. Hameyer ,"High-Performance Adaptive Torque Control for an IPMSM With Real-Time MTPA Operation ", IEEE Trans. on Energy Conv., 32(2): 571-581, June 2017.

[25] Y.-R. Mohamed and T. K. Lee, "Adaptive self-tuning MTPA vector controller for IPMSM drive system," IEEE Trans. Energy Conv., 21(3): 636–644, Sep. 2006.

[26] W. F. Traoré and R. McCann, "Torque measurements in synchronous generators using giant magnetoresistive sensor arrays via the Maxwell stress tensor," IEEE Power & Energy Society General Meeting, pp. 1-5, Jul 2013.

[27] Z. Lin, D. S. Reay, B. W. Williams, and X. He, "Online modeling for switched reluctance motors using B-spline neural networks," IEEE Trans. Ind. Electron., 54(6): 3317-3322, Dec. 2007.

[28] D. Reigosa, Y.G. Kang, M. Martinez, D. Fernandez, J.M. Guerrero and F. Briz, "SPMSMs Sensorless Torque Estimation Using High Frequency Signal Injection", IEEE-ECCE, pp. 2388-2393, Sept. 2019.

[29] J. F. Gieras and M. Wing, "Permanent magnet motor technology: design and application". Second edition 2002.

[30] M. C. Harke, D. Raca, and R. D. Lorenz, "Fast and smooth initial position and magnet polarity estimation of salient and near zero saliency PM synchronous machines," in Proc. IEEE Int. Conf. Elect. Mach. Drives, pp. 1037–1044, May 2005.

[31] S-C. Yang, R.D. Lorenz, "Surface Permanent-Magnet Machine Self-Sensing at Zero and Low Speeds Using Improved Observer for Position, Velocity, and Disturbance Torque Estimation," Trans. on Ind. Appl., 48(1): 151-160, 2012.

[32] J. S. Lee, C. Choi, J. Seok and R. D. Lorenz, "Deadbeat-Direct Torque and Flux Control of Interior Permanent Magnet Synchronous Machines With Discrete Time Stator Current and Stator Flux Linkage Observer," in IEEE Transactions on Industry Applications, 47(4): 1749-1758, July-Aug. 2011.

[33] G. Andreescu, C. I. Pitic, F. Blaabjerg and I. Boldea, "Combined Flux Observer With Signal Injection Enhancement for Wide Speed Range Sensorless Direct Torque Control of IPMSM Drives," IEEE Transactions on Energy Conversion, 23(2): 393-402, June 2008.

[34] T. Sebastian, "Temperature effects on torque production and efficiency of PM motors using NdFeB magnets," IEEE Transactions on Industry Applications, 31(2): 353-357, March-April 1995.

[35] A. Consoli, G. Scarcella, G. Scelba and A. Testa, "Steady-State and Transient Operation of IPMSMs Under Maximum-Torque-per-Ampere Control," IEEE Transactions on Industry Applications, 46(1): 121-129, Jan.-Feb. 2010.

[36] D. Reigosa, D. Fernandez, H. Yoshida, T. Kato and F. Briz "Permanent-Magnet Temperature Estimation in PMSMs Using Pulsating High-Frequency Current Injection," IEEE Trans. on Ind. Appl., 51(4): 3159–3168, July-Aug 2015.

[37] D. Reigosa, D. Fernandez, T. Tanimoto, T. Kato, F. Briz, "Comparative Analysis of BEMF and Pulsating High Frequency Current Injection Methods for PM Temperature Estimation in PMSMs", IEEE Trans. on Power Elect., 32(5): 3691-3699, May 2017.

[38] D. Reigosa, F. Briz, P. García, J. M. Guerrero and M. W. Degner, "Magnet temperature estimation in surface PM machines using high frequency signal injection". IEEE Trans. on Ind. Appl., 46(4): 1468–1475, July-Aug. 2010.

[39] Y-G. Kang, B. Sarlioglu, and R. D. Lorenz, "Saliency based Self-Sensing Enhanced Operating Condition Monitoring using High-Frequency Injection under Intentional Magnetic Saturation," IEEE International Electric Machines and Drives Conference (IEMDC), May 2019.

[40] https://emrax.com

[41] https://www.unitek-industrie-elektronik.de

[42] https://interfaceforce.co.uk/